Polymorphism

DOI: 10.1002/anie.201000680

The Structures of δ-$PdCl_2$ and γ-$PdCl_2$: Phases with Negative Thermal Expansion in One Direction**

Jürgen Evers, Wolfgang Beck, Michael Göbel, Stefanie Jakob, Peter Mayer, Gilbert Oehlinger, Marianne Rotter, and Thomas M. Klapötke*

Dedicated to Professor Rolf Huisgen on the occasion of his 90th birthday

Four modifications of palladium(II) chloride exist at ambient pressure, but only two them, the α- and the β-phase, have been structurally characterized. According to a single-crystal X-ray investigation by Wells[1] in 1938, α-$PdCl_2$ crystallizes in the space-group *Pnnm* with two formula units in the orthorhombic unit cell and forms ribbons of edge connected $PdCl_4$ squares. After more than 70 years it is reasonable to perform a refinement of the Wells structural data with modern diffraction techniques.

β-$PdCl_2$ was detected by Schäfer et al.,[2] its structure was solved in a single-crystal X-ray investigation by Belli Dell'-Amico et al.[3] β-$PdCl_2$ crystallizes with rhombohedric symmetry in space group $R\bar{3}$ with one Pd_6Cl_{12} formula unit in the rhombohedric unit cell. Analogous to Pt_6Cl_{12},[4,5] clusters of Pd_6Cl_{12} build up isolated cubes with $PdCl_4$ squares on their faces. The Pd atoms occupy the center of these faces, the Cl atoms are located at the midst of the edges.

First evidence for the existence of the two other polymorphs was found in 1965 by an X-ray powder investigation of Soulen and Chapell.[6] They established that α-$PdCl_2$ is a high-temperature phase, quite analogous to α-$PtCl_2$. They discovered also a low-temperature phase and published four *d*-values of the powder pattern. This low-temperature phase will be termed γ-$PdCl_2$. Commercially available $PdCl_2$ crystallizes with this structure. In addition, Soulen and Chapell[6] detected a second high-temperature phase by its weak endothermic signal at 504 °C in the thermogram. This phase will be named δ-$PdCl_2$.

To date the structure γ-$PdCl_2$ could not be solved from X-ray powder data. In the thesis of Thiele[7] (1964) a line diagram of the of the Debye–Scherrer X-ray film and a table of 21 θ values were published. The thesis of Klein[8] (1969) contained a table of 17 *d*-values of γ-$PdCl_2$,[6] which were derived from a Guinier-X-ray-film. However, no indexing of these data was given.

The thermogram (Figure 1) shows three endothermic signals of phase transitions at 401 (γ→α), 504 (α→δ), and 683 °C (δ→melt) and confirmed the data of Soulen and Chapell.[6] The peak area of the transition at 504 °C is about 15-times smaller than those at 401 and 683 °C. This result is compatible with a displacive phase transition α→δ involving a small structural realignment. As a result, δ-$PdCl_2$ is not quenchable to ambient temperature and structural investigations must, therefore, be performed in situ between 504 and 683 °C. Figure 1 indicates also that the structural realignment in the phase transitions γ→α and δ→melt are of comparable size. In addition, the phase transition γ→α at 401 °C is the only one that is not reversible. Therefore this phase transition is reconstructive with a great kinetic hindrance. Investigations by Klein[8] showed that at room temperature the transformation rate of the metastable α-$PdCl_2$ is very low. In nine months only 50 % of the α-$PdCl_2$ is transformed into the thermodynamic stable γ-$PdCl_2$.

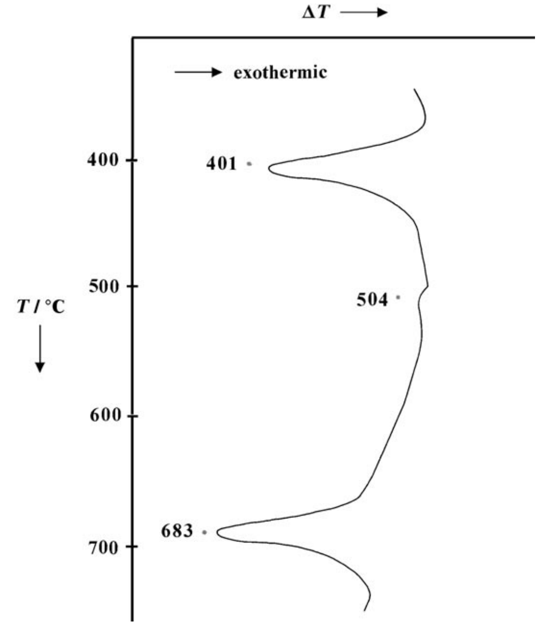

Figure 1. Thermogram of γ-$PdCl_2$ (140 mg, three closed silica glass capillaries, 2.0 mm diameter) under static argon atmosphere. The heating rate is 20°C min^{-1}. The transitions at 504 and 683 °C are reversible on cooling, the transition at 401 °C is not.

---

[*] Prof. Dr. J. Evers, Prof. Dr. W. Beck, Dr. M. Göbel, Dr. S. Jakob, Dr. P. Mayer, G. Oehlinger, M. Rotter, Prof. Dr. T. M. Klapötke
Department für Chemie, Ludwig-Maximilians-Universität München
Butenandtstrasse 5–13, 81377 München (Germany)
Fax: (+49) 89-2180-77950
E-mail: eve@cup.uni-muenchen.de

[**] J.E. thanks Prof. Dr. H. Bärnighausen and Prof. Dr. M. Ruck for valuable comments.

Supporting information for this article is available on the WWW under http://dx.doi.org/10.1002/anie.201000680.

In Table 1 the lattice parameters, the unit cell volume, the positional parameters of the Cl atoms, and the isotropic displacement parameters at four temperatures are summarized for the α phase.[9] In Table 2 distances and angles for this phase are given. A comparison with the data of Wells[1] for α-$PdCl_2$ at 300 K shows that a good agreement is achieved with only small deviations for the palladium and the chlorine atoms (Pd: 0.037, Cl: 0.039 Å).

Table 1: . Single crystal data[9] of α-$PdCl_2$, which is metastable in the investigated temperature range *T* [K].[a]

T	100	200	300	400
a	3.7572(4)	3.7832(6)	3.8115(5)	3.8489(5)
b	10.8941(11)	10.9967(17)	11.0371(13)	11.1329(14)
c	3.3463(3)	3.3513(5)	3.3429(3)	3.3388(3)
V	136.97(2)	139.42(4)	140.63(3)	143.07(3)
x_{Cl}	0.1674(3)	0.1648(4)	0.1627(5)	0.1589(4)
y_{Cl}	0.13309(8)	0.13274(9)	0.13199(11)	0.13138(10)
U_{Pd}	0.0087(1)	0.0158(1)	0.0240(2)	0.0337(1)
U_{Cl}	0.0127(3)	0.0228(3)	0.0352(4)	0.0498(3)

[a] lattice parameters *a*, *b*, *c* [Å], cell volume *V* [Å^3], positional parameters of the chlorine atoms x_{Cl} and y_{Cl}, and the isotropic displacement parameters *U* [Å^2].

Table 2: Interatomic distances [Å] and angles [°] of α-$PdCl_2$ at four temperatures.[9]

T	100	200	300	400
Same ribbon:				
Pd-Cl 4×	2.3016(7)	2.3081(7)	2.3023(9)	2.3022(9)
Cl-Pd 2×	2.3016(7)	2.3081(7)	2.3023(9)	2.3022(9)
Cl-Cl 1×	3.161(1)	3.174(1)	3.167(1)	3.171(1)
Cl-Cl 2×	3.346(1)	3.351(1)	3.343(1)	3.339(1)
Pd-Pd 2×	3.346(1)	3.351(1)	3.343(1)	3.339(1)
Cl-Pd-Cl	93.26(4)	93.10(4)	93.10(5)	92.96(4)
Cl-Pd-Cl	86.74(4)	86.90(4)	86.90(5)	87.04(4)
Neighboring ribbon:				
Cl-Cl 4×	3.580(2)	3.611(2)	3.635(2)	3.670(2)
Cl-Cl 2×	3.757(2)	3.783(2)	3.812(2)	3.849(2)
Pd-Pd 2×	3.757(2)	3.783(2)	3.812(2)	3.849(2)
Cl-Cl 1×	3.828(2)	3.867(2)	3.886(2)	3.931(2)
Pd-Cl 4×	3.832(2)	3.863(2)	3.886(2)	3.925(2)

Figure 2 shows the unit cell of α-$PdCl_2$.[10] With increasing temperature the angle between the ribbons of slightly distorted $PdCl_4$ squares and the *b* axis narrows from −23.5° and +23.5° at 100 K to −22.7° and +22.7° at 400 K. Interestingly, α-$PdCl_2$ shows the anomalous behavior of a "negative thermal expansion (NTE)"[11–13] for the *c* axis with increasing temperature (Table 1). In the temperature range between 100 and 400 K the Pd–Cl distances (Table 2) differ only slightly.

Above 130 °C, structural investigations have been performed on microcrystalline samples of $PdCl_2$ by using the X-ray Guinier technique. At 500 °C the diffractogram indicates a 1:1 mixture of α-$PdCl_2$ and the new δ-$PdCl_2$, at 520 °C the new phase is then obtained as single modification. The Guinier diffractogram of δ-$PdCl_2$ did not show any extinctions, so the space-group could be *P*2, *Pm*, or *P*2/*m*. Using *P*2/*m* the structure could successfully solved.

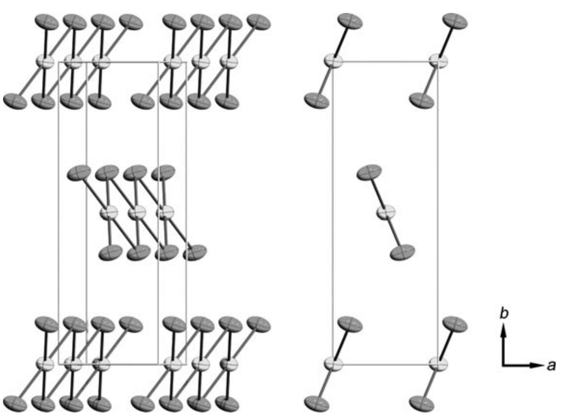

Figure 2. Diamond plots[10] of the α-$PdCl_2$ phase at 400 K[9] with infinite long chains of chloro-bridged square-planar coordinate palladium atoms. The generated ribbons of edge connected $PdCl_4$ squares run parallel to [001] through the edges and the center of the cell. They are symmetrically twisted against the *b* axis (−22.7°, +22.7°). The anisotropic displacement parameters are set at 50% probability.

The crystal structures of α-$PdCl_2$ and of δ-$PdCl_2$ are related to each other in a group–subgroup relation.[15] The monoclinic space group *P*112/*m* (*P*2/*m*) (δ-$PdCl_2$) is a subgroup of the space group *P*2$_1$/*n*2$_1$/*n*2*m* *(Pnnm)* (α-$PdCl_2$). The scheme in Figure 3 shows the group-theory correlation.

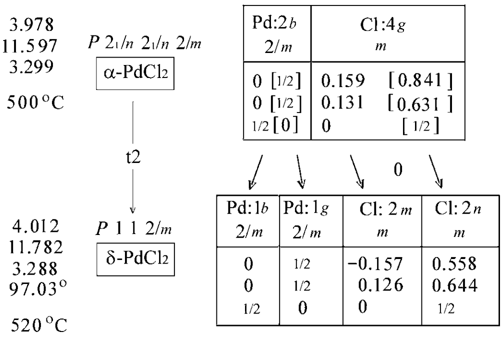

Figure 3. Group-theory relationship between the crystal structures of α- and δ-$PdCl_2$. In a t2 transition the symmetry is reduced. For α-$PdCl_2$ the crystal axes at 500 °C and the positional parameters of the single crystal investigation at 400 K are used,[9] for δ-$PdCl_2$ the data at 520 °C (Table 3) are used.

The transition is "translationengleich" of index 2 (t2). The coordinates of the palladium atoms (0,0,1/2) and (1/2,1/2,0) remain unchanged, those of the chlorine atoms are shifted slightly. Starting with the positional parameters of α-$PdCl_2$ an *R* factor 0.0695 was obtained with all parameters unconstrained. The crystallographic data of the monoclinic high-temperature phase δ-$PdCl_2$ are summarized in Table 3. Figure 4 shows a view along the *c* axis of the monoclinic unit cell of δ-$PdCl_2$ at 520 °C.

Table 3: Crystallographic data of δ-PdCl$_2$ at 793 K and of γ-PdCl$_2$ at 300 K.[25]

Phase	δ-PdCl$_2$	γ-PdCl$_2$
T [K]	793(10)	300(2)
Pearson Symbol	$mP6$	$mP6$
Crystal system	monoclinic	monoclinic
Space group	$P112/m$	$P12_1/c1$
a [Å]	4.012(1)	5.5496(3)
b [Å]	11.782(7)	3.8608(2)
c [Å]	3.288(1)	6.4105(3)
α [°]	90	90
β [°]	90	107.151(2)
γ [°]	97.03(3)	90
V [Å^3]	154.3(1)	131.24(2)
Z	2	2
ρ_{exp} [g cm^{-3}]	–	4.44(5)
ρ_{calcd} [g cm^{-3}]	3.818(2)	4.487(1)
Pd/Wyckoff site	1 Pd(1)/1b (0,0,1/2) 1 Pd(2)/1g (1/2,1/2,0)	2 Pd/2c[a] (0,1/2,0)
Cl/Wyckoff site	2 Cl(1)/2m (x,y,0) (−0.157(8),0.126(1),0)	4 Cl/4e (x,y,z) (0.2550(4),0.2573(7), 0.8141(7))
Cl/Wyckoff Site	2 Cl(2)/2n (x,y,1/2) (0.558(6),0.644(1),1/2)	
U_{Pd} [Å^2]	0.097(3)	0.0083(4)
U_{Cl} [Å^2]	0.120(9)	0.0170(6)

[a] The Pd position is disordered by 30% with a translational vector (0,1/2,0).

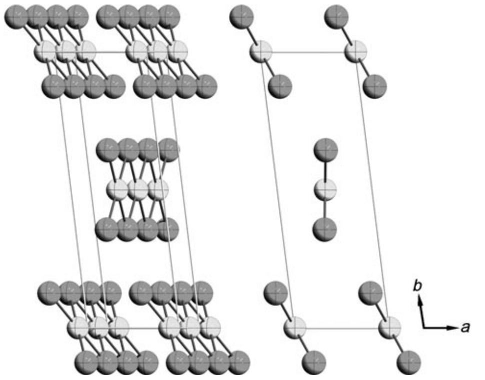

Figure 4. Diamond plots[10] of δ-PdCl$_2$ at 520 °C. Planar ribbons of edge-connected PdCl$_4$ squares run parallel to [001] through the top and bottom edges and the center of the unit cell. The ribbons are asymmetrically twisted against the b axis (−22°, +8°). The high isotropic displacement parameters (U_{Pd} = 0.097(3), U_{Cl} = 0.120(9) Å^2) were derived from the Guinier measurement at 520 °C (Table 3) and represent a 50% probability.

In δ-PdCl$_2$ there are ribbons built up of slightly distorted PdCl$_4$ squares along the c axis as also observed in α-PdCl$_2$. Within the squares the Pd−Cl distances at 520 °C are 2.35(2) Å (4×), the Cl-Pd-Cl angles 89(1) and 91(1)° (both 2×). In α-PdCl$_2$ (space group $Pnnm$) the ribbons run through the corners and the center of the unit cell. They are built up by one crystallographic site and are twisted symmetrically against each other. The structure of δ-PdCl$_2$ (space group $P2/m$) is of lower symmetry (Figure 3). The unit cell contains two independent ribbons which are built up by two crystallographic sites (Table 3, Figure 4). In this case, the ribbons are twisted with two different angles against the b axis. The angle between the ribbons decreases in α-PdCl$_2$ with increasing temperature (100 K: 47.0°; 400 K: 45.4°). In δ-PdCl$_2$ at 793 K this angle is now 30°. Compared to α-PdCl$_2$, in δ-PdCl$_2$ the c axis is longer and it has a larger cell volume and a larger thermal expansion of this volume. Quite uncommon is, however, that the high-temperature phase δ-PdCl$_2$ has a lower symmetry ($P2/m$) than α-PdCl$_2$ ($Pnnm$) which is stable at the lower temperature. The NTE effect is also observed in δ-PdCl$_2$. The c axis contracts from 3.296(3) Å at 777 K (= 504 °C) to 3.266(3) Å at 950 K, and the monoclinic angle narrows from 96.97(4) to 95.55(3)°.

The structure for γ-PdCl$_2$ was solved with high-resolution X-ray Guinier diffractograms with Cu$_{K\alpha_1}$ radiation between 10 and 300 K. γ-PdCl$_2$ crystallizes in a novel structure type in the space group $P2_1/c$ with two formula units in the unit cell. The crystallographic data are summarized in Table 3. According to the Patterson synthesis[16,17] and the Rietveld refinement[18] the Pd position on site 2c (0,1/2,0) (Table 3) is disordered to 30% by a translational vector (0,1/2,0). The Cl position shows no disorder.

Figure 5 shows three views of the low-temperature phase γ-PdCl$_2$: along the twisted b axis and along the c axis with corner-connected PdCl$_4$ squares (Figure 5 a). In this way layers of PdCl$_4$ with W corrugation are built up (Figure 5 b). Figure 5 c shows a view along the b axis of the layers of PdCl$_4$ squares.

In γ-PdCl$_2$ a novel motif connecting PdCl$_4$ squares is realized. In α- and in δ-PdCl$_2$ the ribbons are edge connected, in β-PdCl$_2$ the clusters are corner connected, and in γ-PdCl$_2$ the layers are corner connected. In γ-PdCl$_2$ the arrangement of Cl squares is centered by Pd atoms at (0,1/2,0) and (0,0,1/2) (site 2c) (70%). A second arrangement of Cl squares is realized which are centered by Pd atoms at (0,0,0) and (0,1/2,1/2) (site 2a) (30%). This arrangement leads to the translational disorder of the Pd atoms with the vector (0,1/2,0).

The Pd−Cl distances and the Cl-Pd-Cl angles within the PdCl$_4$ squares of γ-PdCl$_2$ are 2.30(1) und 2.32(1) Å (both 2×) and 88.0(1)s and 92.1(1)° (both 2×). These Pd−Cl distances are comparable to those in α-PdCl$_2$ (2.3016(7)–2.3081(7) Å, at 100–400 K, Table 2), but smaller than that in δ-PdCl$_2$ (2.35(2) Å) at 520 °C. In β-PdCl$_2$ these distances lie between 2.304(1) and 2.312(1) Å and the angles between 89.18(3) und 90.26(9)°.[3] During the transition γ→α, layers of corner-connected PdCl$_4$ squares must be realigned into ribbons of edge-connected PdCl$_4$ squares. For such a reconstructive transition there is no group-subgroup relation as in the case of the transition α→δ. In Table 4 for γ-PdCl$_2$ in the temperature range between 10 and 300 K the lattice parameters a, b, c, β, and the cell volume V are summarized. It is evident that in γ-PdCl$_2$ as also in α-PdCl$_2$ (Table 1) and in δ-PdCl$_2$ (see Figure 6 b) a negative thermal expansion of the c axis occurs. This is the direction in which in γ-PdCl$_2$ the PdCl$_4$ squares are connected to layers (Figure 5 a and c). The NTE effect is much higher in α-PdCl$_2$ and in δ-PdCl$_2$ with edge-connected squares than in γ-PdCl$_2$ with corner-connected squares.

In Figure 6 the change in volume V is plotted as function of temperature for the axes a, b, c. For α-PdCl$_2$ and for

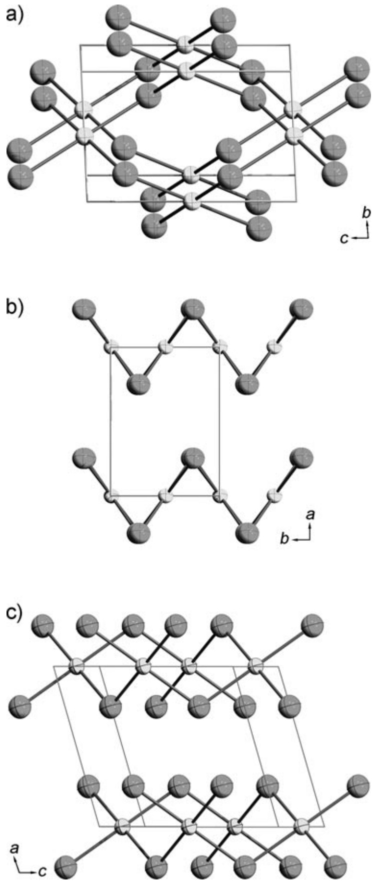

Figure 5. Diamond plots[10] of γ-$PdCl_2$. a) A perspective view along the *a* axis of the monoclinic unit cell. Edge connected $PdCl_4$ squares are built up which are twisted by 69° against each other. b) A view along the *c* axis of the monoclinic unit cell. An arrangement of layers with W corrugation is obtained which is stacked so that the lower atoms are under the gaps in the upper layer. c) A perspective view along the *b* axis of the layers of $PdCl_4$ squares.

Table 4: Lattice parameters [Å], monoclinic angle [°], cell volume [Å³] for γ-$PdCl_2$ in the temperature range 10–300 K, obtained from Guinier diffractograms with $Cu_{K\alpha_1}$ radiation with Rietveld technique.[18]

T [K]	*a*	*b*	*c*	*β*	*V*
10	5.5223(4)	3.8224(2)	6.4194(4)	107.296(3)	129.38(2)
50	5.5252(4)	3.8259(2)	6.4192(4)	107.282(3)	129.57(2)
100	5.5295(4)	3.8321(2)	6.4177(3)	107.254(3)	129.87(2)
150	5.5342(3)	3.8394(2)	6.4151(3)	107.224(3)	130.20(2)
200	5.5387(3)	3.8465(2)	6.4131(3)	107.197(3)	130.52(2)
250	5.5437(3)	3.8534(2)	6.4119(3)	107.169(3)	130.87(2)
300	5.5496(3)	3.8608(2)	6.4107(3)	107.151(3)	131.25(2)

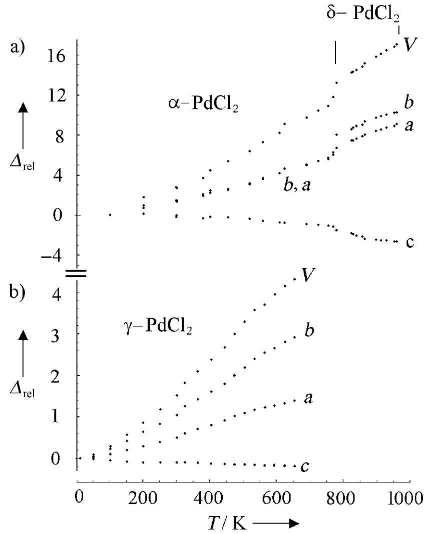

Figure 6. Relative change Δ_{rel} of the volume *V* and the crystal axes *a*, *b*, and *c* with variation of the temperature. a) For α- and δ-$PdCl_2$ *V* (+17.0%), *a* (+9.1%), and *b* (+10.3%) increase in the temperature range from 100 to 959 K, contrary to *c* (−2.7%) which contracts as a result of the NTE effect. b) For γ-$PdCl_2$ *V* (+4.1%), *a* (+1.3%), and *b* (+2.8%) increase in the temperature range from 10 to 674 K, contrary to *c* (−0.3%) which contracts as a result of the NTE effect.

δ-$PdCl_2$ (Figure 6a) the values were normalized to 100 K, for γ-$PdCl_2$ (Figure 6b) to those at 10 K. It is evident, that in α-$PdCl_2$ and also in δ-$PdCl_2$ the volume *V* as well as the axes *a* and *b* increase with increasing temperature, but the *c* axis contracts owing to the NTE effect (Figure 6a).

To investigate the stability relations between α-, β-, γ-, and δ-$PdCl_2$, the total energies for one $PdCl_2$ formula unit were calculated as a function of the volume, using density functional theory (DFT) with the program WIEN2k [19] (Figure 7).[20] At the intersection of the graphs for the two high-temperature phases α and δ ($S_{\alpha\text{-}\delta}$, Figure 7) volume and energy are equal. At smaller volume the α-phase is stable, at higher volume, the δ-phase. Clearly smaller energies than those for α and δ are calculated for the phases γ and β, for which β is the lowest in energy. Single crystals of β-$PdCl_2$ can be prepared from $[Pd_3(CH_3COO)_6]$ in aromatic solvents by addition of glacial acetic acid and perchloric acid and subsequent treatment with CO[21] or, alternatively, by decomposition of the complex $[Pd_2Cl_4(CO)_2]$ in $SOCl_2$.[3] In contrast, treating Pd metal with aqua regia, evaporation of the resulting solution, and subsequent heating the dry palladium chloride to 150 °C results in microcrystalline γ-$PdCl_2$.[7,8]

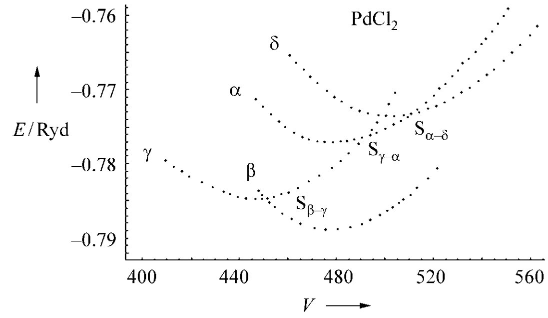

Figure 7. Total energy for one formula unit of $PdCl_2$ calculated with the program WIEN2k[19,20] as function of the volume for the four polymorphic phases.

Experimental Section

Single crystals of α-$PdCl_2$ were obtained by sublimation of commercially available $PdCl_2$ (ca. 500 mg; STREM Chemicals, No. 46–1850) at 670 °C in an under vacuum closed and before use degassed silica glass tube (length 10 cm, diameter 1 cm). In the temperature range 500–510 °C (phase transition $\delta \rightarrow \alpha$ at 504 °C) the tube was cooled slowly with 2°C$\,h^{-1}$, then from 470 °C to room temperature over a day.

The single-crystal investigations of α-$PdCl_2$ were performed on an Oxford XCalibur3 diffractometer with Enhance $Mo_{K\alpha}$ radiation source at 100, 200, 300, and 400 K. The absorption correction was calculated with the program "Scale3 Abspack" ("Spherical Harmonics") which is implemented in the software of the Oxford diffractometer. The structures have been refined with SHELXL-97[22] with the method of least-squares in full-matrix technique for F^2.

The structural investigations on powders of $PdCl_2$ were performed on two different Guinier diffractometers (HUBER Diffraktionstechnik). For the high-temperature measurements (300 to 960 K) a HUBER G644-diffractometer with heating equipment (monochromatic $Mo_{K\alpha_1}$ radiation, $\lambda = 0.7093$ Å, 750 data points between 6.00 and 36.00°, 2θ, closed silica glass capillary, 0.5 mm diameter, with Pd powder as internal standard[23]), for the low-temperature measurements (10 to 300 K) a Guinier diffractometer HUBER G670 with low-temperature equipment G670.4 (monochromatic $Cu_{K\alpha_1}$ radiation, $\lambda = 1.54056$ Å, 17200 data points between 14.000 and 100.000°, 2θ, powder sample finely distributed between two foils of a 6 μm thin polyacetate[24]).

The indexing of 20 reflections of the novel high-temperature phase δ-$PdCl_2$ with the program DICVOL[14] resulted in a monoclinic unit cell with $a = 4.0514$, $b = 3.2849$, $c = 11.864$ Å and $\beta = 96.56°$ (reliability coefficient $F_{20} = 25$). To obtain a good comparison with α-$PdCl_2$ this cell with b as the monoclinic axis was transformed into that with c as the monoclinic axis. The diffractograms of the low-temperature phase were also indexed with the program DICVOL with high reliability coefficients ($M_{20} = 22$). With these lattice parameters the X-ray powder data of Soulen and Chapell[6] and of Thiele[7] could be indexed as pure phases. An automatic indexing of the data of the Guinier film of Klein[8] is only successful if four reflections of a second phase are omitted. The reflections $h0l$ for $l \neq 2n$ and $0k0$ for $k \neq 2n$ fix the space group $P2_1/c$ for γ-$PdCl_2$. The structure solution was performed with the program FullProf[18] in Rietveld technique. Pattern Matching Analysis of the Guinier diffractogram with $Cu_{K\alpha_1}$ radiation at 300 K with the lattice parameters of the DICVOL indexing lead to low R factors ($R = 0.0434$, $Bragg\text{-}R = 0.0077$) and also to the F_{hkl} data. A Patterson synthesis of these data with the program SHELXS-97[16] resulted in the interatomic vectors[17] Pd–Pd, Pd–Cl, and Cl–Cl. Up to a height of two Cl–Cl vectors the Patterson synthesis contains, beside the origin vector, seven additional interatomic vectors, which can all be interpreted with the structure of γ-$PdCl_2$ (Table 3). The third-strongest vector (0,1/2,0) with 1.93 Å causes problems because in γ-$PdCl_2$ the shortest Pd–Cl distances realizable should be approximately 2.30 Å. Weak reflections allowing another indexing could not be found in the highly resolved Guinier diffractograms. The vector (0,1/2,0) was than interpreted as translational disorder of 30% of the Pd atoms. With the $F_{hkl,\mathrm{obs}}$ data, obtained after Rietveld refinement ($R = 0.0584$ and $R_p = 0.0818$), an R factor of 0.1142 for 130 $F_{\mathrm{obs}} > 4\sigma$ was obtained with the program SHELXL-97.[22] A difference Fourier synthesis showed only smaller peaks of disordered atoms without any plausible interpretation. Disorder in the Guinier diffractogram of γ-$PdCl_2$ is also derived from the high background of the reflection group between 27 to 29° (2θ).

The single-crystal X-ray data of α-$PdCl_2$ are available free of charge at the Fachinformationszentrum (FIZ) Karlsruhe.[9] The data of the X-ray powder measurements on α-$PdCl_2$ at 480 °C, on δ-$PdCl_2$ at 520 °C, and on γ-$PdCl_2$ at 300 K are also available free of charge at FIZ Karlsruhe.[25] The thermoanalytical investigations were performed on a LINSEIS differential thermoanalytic equipment under a protective atmosphere of argon with PtRh thermoelements (140 mg commercially available γ-$PdCl_2$, closed in three short silica X-ray capillaries (2.0 mm diameter, heating rate 20°C$\,min^{-1}$).

Received: February 4, 2010
Revised: April 20, 2010

Keywords: density functional calculations · palladium · phase transitions · structure determination · X-ray diffraction

---

[1] A. F. Wells, *Z. Kristallogr. A* **1938**, *100*, 189.

[2] H. Schäfer, U. Wiese, K. Rinke, K. Brendel, *Angew. Chem.* **1967**, *79*, 244; *Angew. Chem. Int. Ed. Engl.* **1967**, *6*, 253.

[3] D. Belli Dell'Amico, F. Calderazzo, F. Machetti, S. Ramello, *Angew. Chem.* **1996**, *108*, 1430; *Angew. Chem. Int. Ed. Engl.* **1996**, *35*, 1331.

[4] B. Krebs, C. Brendel, H. Schäfer, *Z. Anorg. Allg. Chem.* **1988**, *561*, 119.

[5] a) K. Brodersen, G. Thiele, H. G. von Schnering, *Z. Anorg. Allg. Chem.* **1965**, *337*, 120; b) G. Thiele, K. Brodersen, *Fortschr. Chem. Forsch.* **1968**, *10*, 631.

[6] J. R. Soulen, W. H. Chapell, *J. Phys. Chem.* **1965**, *69*, 3669.

[7] G. Thiele, *Dissertation*, Rheinisch-Westfälische Technische Hochschule Aachen, **1964**.

[8] M. Klein, *Dissertation*, Universität Münster, **1969**.

[9] Further details on the crystal structure investigation may be obtained from the Fachinformationszentrum Karlsruhe, 76344 Eggenstein-Leopoldshafen, Germany (fax: (+49) 7247-808-666; e-mail: crysdata@fiz-karlsruhe.de), on quoting the depository numbers CSD-421213, -421214, -421215, and CSD-421216.

[10] K. Brandenburg, *Visual Crystal Structure Information System*, Diamond2, Crystal Impact GbR, Bonn, **1999**.

[11] K. W. Chapman, P. J. Chupas, C. J. Kepert, *J. Am. Chem. Soc.* **2005**, *127*, 15630.

[12] A. L. Goodwin, C. J. Kepert, *Phys. Rev. B* **2005**, *71*, 140301.

[13] S. J. Hibble, A. C. Hannon, S. M. Cheyne, *Inorg. Chem.* **2003**, *42*, 4724.

[14] A. Boultif, D. Louer, *J. Appl. Crystallogr.* **2004**, *37*, 724.

[15] U. Müller, *Z. Anorg. Allg. Chem.* **2004**, *630*, 1519.

[16] G. M. Sheldrick, *SHELXS-97*, *Program for Crystal Structure Solution*, Universität Göttingen, **1997**.

[17] Patterson synthesis (calculated peak height Pd–Pd 392, Pd–Cl 145, Cl–Cl 56, to 2 × Cl–Cl): **Nr.**: coordinates X, Y, Z/peak/vector/interpretation: **No.1**: 0.0000, 0.0000, 0.0000/999/0.00/origin; **No. 2**: 0.0000, 0.0000, 0.5000/670/3.20/Pd_{11}-Pd_{22}, Pd_{21}-Pd_{12},Cl_{11}-Cl_{14}, Cl_{12}-Cl_{13}; **No.3**: 0.0000, 0.5000, 0.5000/601/3.74/Pd_{11}-Pd_{12}, Pd_{21}-Pd_{22}; **No.4**: 0.0000, 0.5000, 0.0000/395/1.93/Pd_{11}-Pd_{21}, Pd_{12}-Pd_{22}; **No.5**: 0.2725, 0.2524, 0.3181/350/2.35/Cl_{11}-Pd_{12}, Cl_{12}-Pd_{21}; **No.6**: 0.2707, 0.2485, 0.8188/349/2.34/Cl_{12}-Pd_{12}, Cl_{13}-Pd_{21}; **No.7**: 0.4756, 0.5000, 0.3717/140/3.54/Cl_{12}-Cl_{14}, Cl_{11}-Cl_{13}; **No.8**: 0.4587, 0.5000, 0.8737/108/3.45/Cl_{11}-Cl_{12}, Cl_{13}-Cl_{14}; coordinates: Pd_{11}: (0,1/2,0); Pd_{12}: (0,0,1/2); Pd_{21}: (0,0,0); Pd_{22}: (0,1/2,1/2); Cl_{11}: (0.255,0.257,0.814); Cl_{12}: (0.745,0.757,0.686); Cl_{13}: (0.745,0.743,0.186); Cl_{14}: (0.255,0.253,0.314).

[18] J. R. Rodriguez-Carvajal, *FullProf*, *A Program for Rietveld Refinement and Pattern Matching Analysis*, Abstracts of the Satellite Meeting on Powder Diffraction of XV Congress of the IUCr, Toulouse, France **1990**; International Union of Crystallography, Chester, UK, **1990**, p. 127.

[19] P. Blaha, K. Schwarz, G. Madsen, D. Kvasnicka, J. Luitz, *WIEN2k*, *An Augmented Plane Wave Plus Local Orbitals Program for Calculating Crystal Properties*, Vienna University of Technology, Institute of Materials Chemistry, Austria, **2001**.

[20] 23875 Ryd have to be added to the energy values on the ordinate in Figure 7. For the stability of the phases the differences

between the total energies is important; the summand 23875 Ryd is then neglected.

[21] A. Yatsimirski, R. Ugo, *Inorg. Chem.* **1983**, *22*, 1395.

[22] G. M. Sheldrick, *SHELXL-97, Program for Crystal Structure Refinement*, Universität, Göttingen, **1997**.

[23] R. H. Schröder, N. Schmitz-Pranghe, R. Kohlhaas, *Z. Metallk.* **1972**, *63*, 12.

[24] S. Jakob, Dissertation, Ludwig-Maximilians-Universität München, **2007**.

[25] Further details on the crystal structure investigation may be obtained from the Fachinformationszentrum Karlsruhe, 76344 Eggenstein-Leopoldshafen, Germany (fax: (+49) 7247-808-666; e-mail: crysdata@fiz-karlsruhe.de), on quoting the depository numbers CSD-421219, -421220 and -421221.